An ETHYLENE RESPONSE FACTOR-MYB Transcription Complex Regulates Furaneol Biosynthesis by Activating *QUINONE OXIDOREDUCTASE* Expression in Strawberry[1]

Yuanyuan Zhang,[a,2] Xueren Yin,[a,b,c,2] Yuwei Xiao,[a] Zuying Zhang,[a] Shaojia Li,[a] Xiaofen Liu,[a] Bo Zhang,[a,b,c] Xiaofang Yang,[d] Donald Grierson,[a,e] Guihua Jiang,[d,3,4] Harry J. Klee,[a,f,3,4] and Kunsong Chen[a,b,c,3,4]

[a]College of Agriculture and Biotechnology, Zhejiang University, Zijingang Campus, Hangzhou 310058, People's Republic of China

[b]Zhejiang Provincial Key Laboratory of Horticultural Plant Integrative Biology, Zhejiang University, Zijingang Campus, Hangzhou 310058, People's Republic of China

[c]State Agriculture Ministry Laboratory of Horticultural Plant Growth, Development and Quality Improvement, Zhejiang University, Zijingang Campus, Hangzhou 310058, People's Republic of China

[d]Institute of Horticulture, Zhejiang Academy of Agricultural Sciences, Hangzhou 310021, People's Republic of China

[e]Division of Plant and Crop Sciences, School of Biosciences, University of Nottingham, Sutton Bonington Campus, Loughborough LE12 5RD, United Kingdom

[f]Horticultural Sciences, Plant Innovation Center, Genetics Institute, University of Florida, Gainesville, Florida 32611

ORCID IDs: 0000-0003-4207-561X (Y.Z.); 0000-0002-1282-4432 (X.Y.); 0000-0002-3509-4399 (Y.X.); 0000-0001-6602-5559 (Z.Z.); 0000-0001-8702-5590 (S.L.); 0000-0003-1612-0704 (X.L.); 0000-0001-8181-9111 (B.Z.); 0000-0001-8280-3509 (X.Y.); 0000-0002-2238-8072 (D.G.); 0000-0003-2367-1651 (G.J.); 0000-0003-2874-2383 (K.C.)

4-Hydroxy-2,5-dimethyl-3(2H)-furanone is a major contributor to the aroma of strawberry (*Fragaria* × *ananassa*) fruit, and the last step in its biosynthesis is catalyzed by strawberry quinone oxidoreductase (FaQR). Here, an ethylene response factor (FaERF#9) was characterized as a positive regulator of the *FaQR* promoter. Linear regression analysis indicated that *FaERF#9* transcript levels were correlated significantly with both *FaQR* transcripts and furanone content in different strawberry cultivars. Transient overexpression of *FaERF#9* in strawberry fruit significantly increased *FaQR* expression and furaneol production. Yeast one-hybrid assays, however, indicated that FaERF#9 by itself did not bind to the *FaQR* promoter. An MYB transcription factor (FaMYB98) identified in yeast one-hybrid screening of the strawberry cDNA library was capable of both binding to the promoter and activating the transcription of *FaQR* by ~5.6-fold. Yeast two-hybrid assay and bimolecular fluorescence complementation confirmed a direct protein-protein interaction between FaERF#9 and FaMYB98, and in combination, they activated the *FaQR* promoter 14-fold in transactivation assays. These results indicate that an ERF-MYB complex containing FaERF#9 and FaMYB98 activates the *FaQR* promoter and up-regulates 4-hydroxy-2,5-dimethyl-3(2H)-furanone biosynthesis in strawberry.

Introduction

Strawberry (*Fragaria* × *ananassa*) is an economically important, globally popular and attractive fruit with nutritional benefits for human health. An important feature of its appeal is a unique fragrance, with more than 360 different volatile compounds detected in ripe fruit (Ménager et al., 2004; Jetti et al., 2007). These volatiles include alcohols, organic acids, aldehydes, terpenes, lactones, esters, aromatic hydrocarbons, furans, and others (Zabetakis and Holden, 1997). Sensory evaluation indicates that terpenes confer on strawberry a fresh orange smell, aldehydes generate an herbal flavor, γ-decalactone is peach like, esters are fruity, and 4-hydroxy-2,5-dimethyl-3(2)H-furanone (HDMF) and 2,5-dimethyl-4-methoxy-3(2)H-furanone (DMMF) generate a caramel-like aroma (Pyysalo et al., 1979; Larsen and Poll, 1992). HDMF and DMMF belong to an uncommon group of chemicals with a 2,5-dimethyl-3(2H)-furanone structure, and such compounds possess special odor properties (Schwab and Roscher, 1997). They are found at trace levels in various fruits, including raspberry (*Rubus idaeus*), some grape (*Vitis vinifera*) cultivars, and tomato (*Solanum lycopersicum*). They are particularly abundant in strawberry and pineapple (*Ananas comosus*; Schwab, 2013; Wüst, 2017).

[1]This research was supported by The National Key Research and Development Program (2016YFD0400101), The Project of the Science and Technology Department of Zhejiang Province (2016C04001), and The 111 Project (B17039).

[2]These authors contributed equally to the article.

[3]Author for contact: akun@zju.edu.cn.

[4]Senior author.

The author responsible for distribution of materials integral to the findings presented in this article in accordance with the policy described in the Instructions for Authors (www.plantphysiol.org) is: Kunsong Chen (akun@zju.edu.cn).

www.plantphysiol.org/cgi/doi/10.1104/pp.18.00598

HDMF is one of the most important volatiles distinguishing strawberry from other fruits (Larsen and Poll, 1992; Schwab and Roscher, 1997) and is significantly correlated with perceived strawberry fruit intensity (Schwieterman et al., 2014). Thus, strawberry is an important model for investigating the regulation of furaneol biosynthesis, and knowledge of the factors controlling its synthesis is highly desirable for targeting flavor improvement.

HDMF and its methyl ether, DMMF, have been investigated extensively in research on flavor analyses, chemical synthesis, and natural product formation in both microbes and plants (Zabetakis et al., 1999; Schwab, 2013). The first plant studies on the biosynthesis of HDMF used strawberry fruit to investigate potential precursors of furaneol biosynthesis (Pisarnitskii et al., 1992), and D-Fru-1,6-diphosphate was identified as the natural precursor of HDMF and DMMF (Roscher et al., 1998; Schwab, 1998). The immediate precursor of HDMF in strawberry was shown to be 4-hydroxy-5-methyl-2-methylene-3(2H)-furanone, and strawberry quinone oxidoreductase (FaQR, later renamed as FaEO) was identified as the enzyme responsible for reduction of the α,β-unsaturated bond of 4-hydroxy-5-methyl-2-methylene-3(2H)-furanone to form the aroma-active compound HDMF (Raab et al., 2006; Klein et al., 2007). An *O*-methyltransferase, FaOMT, subsequently generates DMMF by the methylation of HDMF (Wein et al., 2002). HDMF also can be metabolized to 2,5-dimethyl-4-hydroxy-2*H*-furan-3-one glucoside (HDMF-glucoside) by a UDP-dependent glycosyltransferase (UGT71K3) and further malonylated into 2,5-dimethyl-4-hydroxy-2*H*-furan-3-one 6′-*O*-malonyl-β-D-glucopyranoside (HDMF malonyl-glucoside) in strawberry fruit (Roscher et al., 1996; Song et al., 2016). The biosynthetic pathway of HDMF in other plants is similar to that in strawberry. Genes with homology to *FaQR* have been identified in tomato (*SlEO*) and mango (*Mangifera indica*; *MiEO*; Klein et al., 2007; Kulkarni et al., 2013).

As an NADH-dependent enone oxidoreductase protein, FaQR exhibits *o*-quinone oxidoreductase activity (Raab et al., 2006). *FaQR* mRNA accumulates in fruit parenchyma tissues but is absent in vascular tissues, and *FaQR* is expressed mainly in the late stages of fruit growth and ripening, paralleling furaneol production in the fruit (Raab et al., 2006). FaQR is responsive to environmental stimuli associated with furaneol production, and in the dark, cv Sweet Charlie strawberry fruits have higher levels of *FaQR* expression and HDMF production at 25°C than at 15°C (Fu et al., 2017); in contrast, the concentration of furanones and the abundance of FaQR protein under low-temperature storage are significantly lower than under room-temperature storage (Li et al., 2015). Thus, the regulation of *FaQR* is important for manipulating furaneol content. Although it is assumed that transcription factors control the expression of genes involved in volatile production in plants, no such factors regulating *FaQR* or other furanone biosynthetic genes have been identified.

Different members of the largely plant-specific AP2/ERF gene family (Weirauch and Hughes, 2011) have diverse functions in plant growth, development, and stress responses (Agarwal et al., 2010; Zhu et al., 2010; Licausi et al., 2013). In recent years, several *AP2/ERF* genes have been reported to regulate aspects of fruit quality (Xie et al., 2016), including fruit aroma. For example, *CitAP2.10* is associated with the synthesis of (+)-valencene in Newhall orange (*Citrus sinensis*), acting via the regulation of *CsTPS1* (Shen et al., 2016); *CitERF71* was shown to bind physically to the *CsTPS16* promoter and contribute to the synthesis of *E*-geraniol in citrus fruit (Li et al., 2017b). These observations raised the possibility that *FaQR* also might be a target for a member of the AP2/ERF family and that ERFs also might control furaneol biosynthesis.

In this study, screening of the strawberry AP2/ERF gene family led to the identification of *FaERF#9* as an activator of *FaQR*; however, it did not bind directly to the promoter. A parallel search for proteins that directly bind the *FaQR* promoter using yeast one-hybrid screening identified a second factor, FaMYB98, which was capable of interacting physically with the *FaQR* promoter. FaMYB98 interacts physically with FaERF#9, and transient expression assays demonstrated a synergistic effect on *FaQR* expression and furanone synthesis.

RESULTS

Changes in the Content of Both Furanones and the Activity of Their Biosynthetic Genes in Strawberry Fruit

Fruits of cv Yuexin at four developmental and ripening stages (G, green; T, turning; IR, intermediate red; R, full red) were harvested (Fig. 1), and the determination of HDMF levels indicated a major increase from about 0.65 μg g^{-1} fruit at the IR stage to 3.46 μg g^{-1} fruit at the R stage in the apical section, implying that furaneol accumulation was closely related to color change and ripening (Fig. 1). Furaneol levels were higher in the apical section than in the basal section. HDMF could not be detected at the IR stage in the basal section, but the amount increased at the R stage to 1.42 μg g^{-1} fruit. Differences also were found for DMMF, with the relative content in the apical section being 0.18 μg g^{-1} at the R stage, compared with 0.08 μg g^{-1} in the basal section at the same stage.

Measurement of mRNA levels by reverse transcription quantitative PCR (RT-qPCR) indicated that the transcript levels of both *FaQR* (GenBank accession no. AY158836.1) and *FaOMT* (GenBank accession no. AF220491.2) increased throughout ripening (Fig. 1). Comparison of the expression of these genes showed that the transcript levels of *FaQR* and *FaOMT* increased significantly as early as the T stage in basal fruit sections, and for each gene over half of the peak transcript abundance occurred as early as the IR stage in the apical section, while for the basal section it was in the R stage, indicating a gradient of gene expression and volatile production from apex to base of the fruit during ripening.

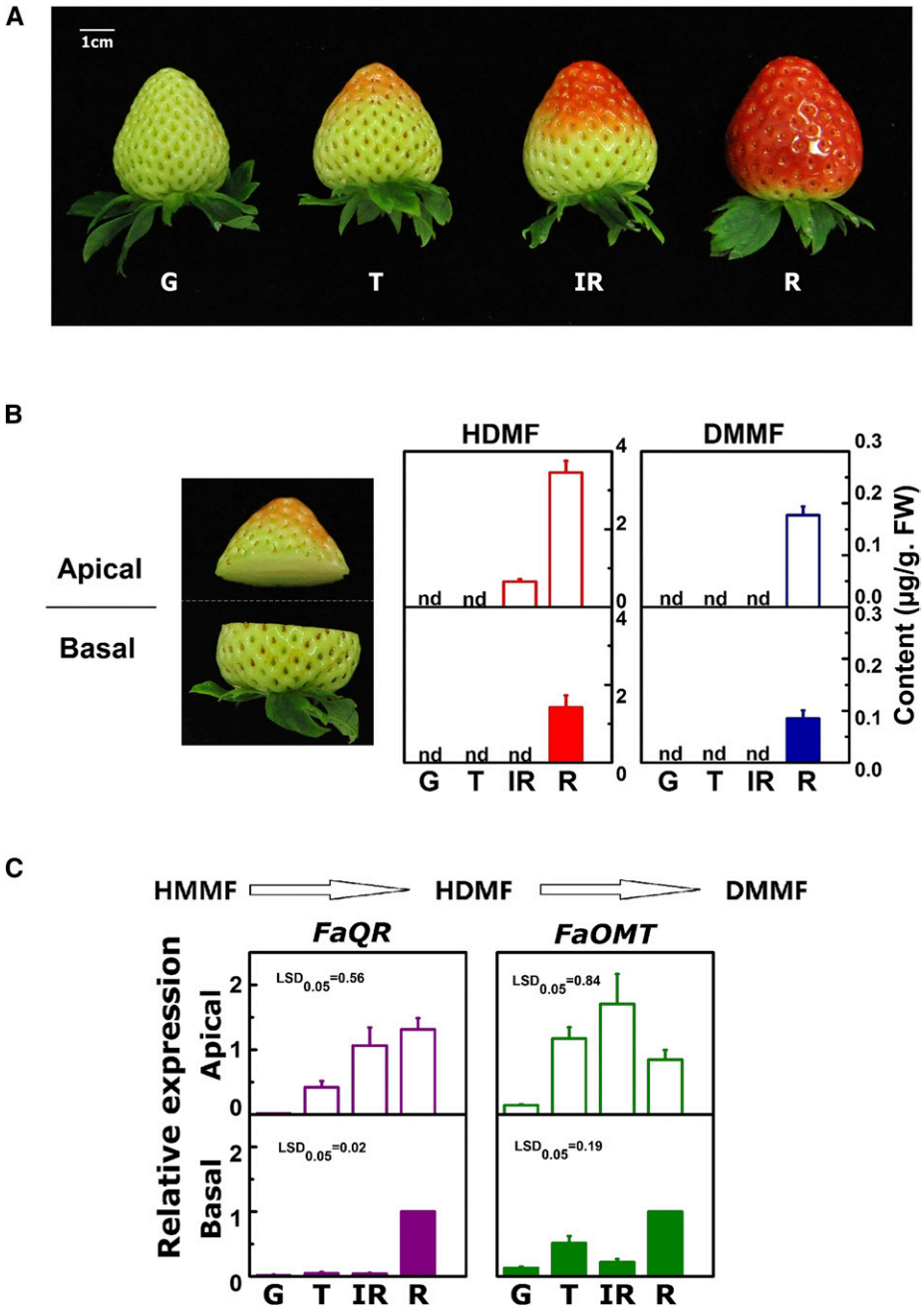

Figure 1. Changes in furanone content and furanone biosynthetic genes during strawberry (cv Yuexin) fruit development and ripening. A, Fruits were collected at four ripening stages: G, T, IR, and R. B, Changes in the contents of furaneol (HDMF) and mesifurane (DMMF). HDMF content was calculated using a standard curve of HDMF, while DMMF content was calculated with an internal standard as the reference. FW, Fresh weight. C, Expression levels of *FaQR* and *FaOMT*. The expression levels of each gene were calculated relative to corresponding values in the basal section at the R stage. SE values were calculated from three replicates, and LSD values were calculated at $P = 0.05$.

Genome-Wide Identification of the AP2/ERF Gene Family in Strawberry

Coding sequences of 120 nonredundant *FaAP2/ERF* genes were isolated and identified from cv Yuexin strawberry, and a systematic nomenclature for the AP2/ERF family genes was used to distinguish the members based on the structural features defined previously (Supplemental Table S1; Shigyo and Ito, 2004; Nakano et al., 2006; Licausi et al., 2013). CD-search analysis showed that this superfamily consisted of 95 ERFs, 18 AP2 and AP6 RAV family members, and one soloist member (Supplemental Table S2). A phy-

logenetic analysis of the strawberry and Arabidopsis (*Arabidopsis thaliana*) AP2/ERF members is shown in Supplemental Figure S1, with the 120 *AP2/ERF* genes divided into three major groups (ERF, AP2, and RAV) and a soloist and the ERF family being divided further into 10 groups (groups I–X in Supplemental Table S1).

We performed a dual-luciferase assay to determine the ability of 116 FaAP2/ERF members to activate transcription from the promoter of *FaQR*. The results indicated that about 12 members (mainly belonging to the ERF and RAV families) showed a significant activation effect on the *FaQR* promoter, while the remaining members showed very limited effects (Fig. 2). The relative activity of only the following 12 *FaAP2/ERF* transcripts reached the threshold value set at 2: *FaERF#8/FaERF#9* (group II), *FaERF#27/FaERF#29/FaERF#31/FaERF#32* (group IV), *FaERF#37/FaERF#38* (group V), *FaERF#62/FaERF#64* (group VIII), *FaERF#68* (group IX), and *FaRAV4* (Fig. 2). Of these, FaERF#9 exhibited the highest activation effect on the *FaQR* promoter (4.66-fold; Fig. 2). The strawberry *FaERF#9* cDNA is 699 bp long, and ExPASy Compute pI/Mw tool analysis indicated that this gene encodes a 232-amino acid protein with a calculated molecular mass of 25.4 kD and a pI of 5.6.

FaERF#9 Expression Pattern and Subcellular Localization

To further explore the connections between AP2/ERFs and furaneol biosynthesis, we obtained the transcript profiles of the *AP2/ERF* genes in strawberry fruit samples at different fruit developmental and ripening stages by RT-qPCR, excluding genes with very low abundance in the fruit samples. The results, presented as a heat map (Supplemental Fig. S2), demonstrate that these genes displayed various expression patterns in both the apical and basal sections, and by analyzing the expression patterns of the members indicated as activators in the dual-luciferase assay, we found that only a few genes, including *FaERF#8*, *FaERF#9*, *FaERF#27*, *FaERF#32*, and *FaERF#37*, were up-regulated during ripening stages, and their expression correlated with furaneol accumulation in the fruit (Fig. 1). Furthermore, the expression patterns of the up-regulated genes in the apical and basal sections showed that one *ERF* gene, *FaERF#9*, not only showed an up-regulation pattern in both sections but its expression in the apical section occurred ahead of that in the basal section (Fig. 3), consistent with the actual changes in furaneol content (Fig. 1) and the expression pattern of *FaQR* (Fig. 1). The subcellular localization of FaERF#9 was predicted to be in the nucleus using the WoLF PSORT program. In experimental tests, 35S-FaERF#9-GFP showed strong fluorescence in the nucleus, and the green signal merged with the red fluorescence signal of the mCherry nucleus marker in tobacco plants (Fig. 3).

Transient Overexpression of *FaERF#9* in Strawberry

The expression of *FaERF#9* in agroinfiltrated fruits was analyzed by performing RT-qPCR on day 7 after

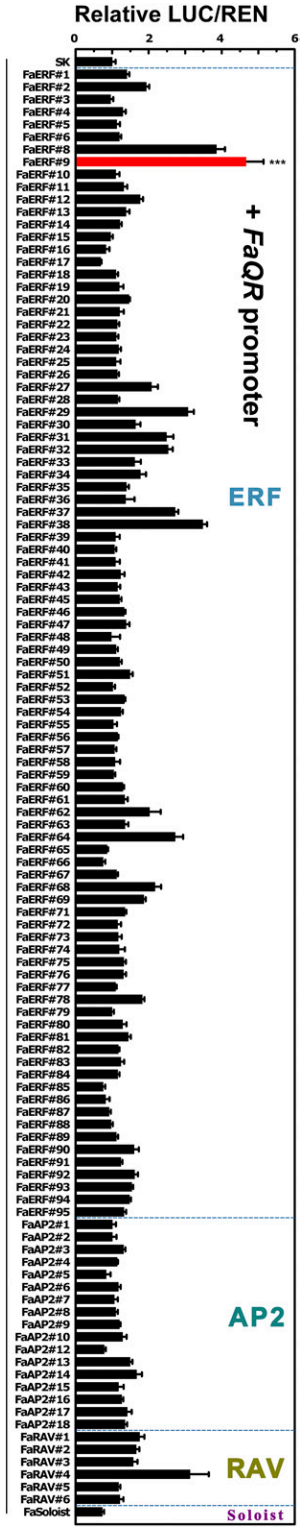

Figure 2. Regulatory effects of *FaAP2/ERF* on the promoter of *FaQR*. Firefly luciferase/*Renilla* luciferase (LUC/REN) values of the empty vector on the *FaQR* promoter were used as the calibrator, set as 1, and SE values were calculated from five replicates. Statistical significance was determined by Student's two-tailed *t* test (***, $P < 0.001$).

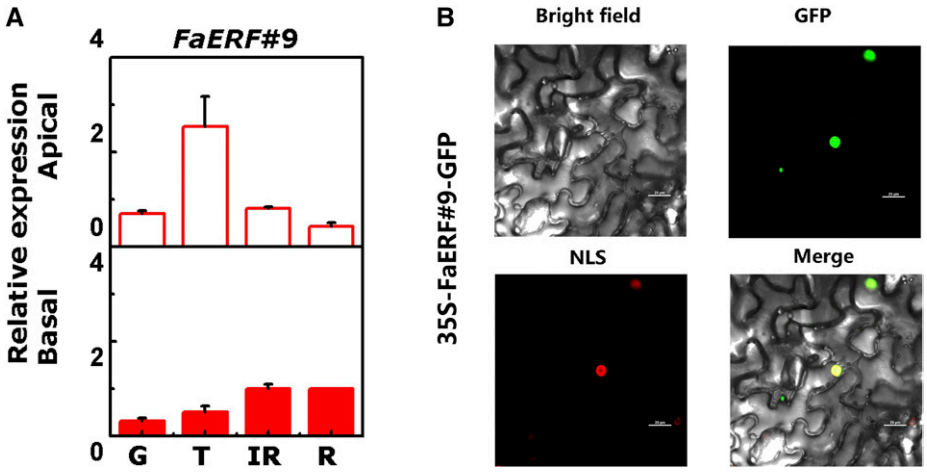

Figure 3. Expression and the subcellular localization of *FaERF#9*. A, Expression levels were calculated relative to the levels in the basal section at the R stage. B, Subcellular localization analysis was performed in tobacco leaves. The tobacco used in the assay was stably transformed with a specific nucleus-localized red fluorescent protein construct, and the red fluorescence indicates the nucleus-localized signal (NLS). SE values were calculated from three replicates. Bars = 25 μm.

infiltration, by which time they had reached the IR or R stage, and the results showed that the transcript levels were significantly higher (5.2-fold) than in control fruits (Fig. 4). The expression of *FaQR* was examined in the same fruits, and the transcript abundance also increased 2.2-fold. The relative content of HDMF in the *FaERF#9*-overexpressing fruits was 0.08 μg g^{-1} fruit and undetectable in the control fruits (Fig. 4). The relative content of DMMF in the overexpressing fruits also was increased significantly, to 0.38 μg g^{-1} fruit compared with 0.04 μg g^{-1} fruit in the control (Fig. 4). These observations provide direct evidence for a regulatory role for FaERF#9 in promoting FaQR biosynthesis and activity in ripening strawberry fruit. Taken together, these results indicate that, by activating the transcription of *FaQR*, *FaERF#9* functions as a positive regulator in furaneol biosynthesis.

Correlation of *FaERF#9* Expression and *FaQR* Transcript Profiles

Gas chromatography-mass spectrometry (GC-MS) quantification showed that furanones are distributed in variable levels among different strawberry cultivars (Supplemental Fig. S3). The transcript profiles of *FaQR* and *FaERF#9* in fruits of different cultivars were measured, and linear regression analysis was performed. In the cultivars, the changes in *FaQR* transcripts correlated positively with those in *FaERF#9* transcripts ($r = 0.79$, $P < 0.01$; Fig. 5). In addition, *FaERF#9* transcript levels also correlated with furanone content across cultivars (Fig. 5).

FaERF#9 Is an Indirect Regulator of the *FaQR* Promoter and Acts via Protein-Protein Interaction with FaMYB98

Although the results of the dual-luciferase assay, expression analysis, transient overexpression, and correlation analysis all were consistent with the suggestion that FaERF#9 regulates transcript abundance by acting on the *FaQR* promoter, a yeast one-hybrid

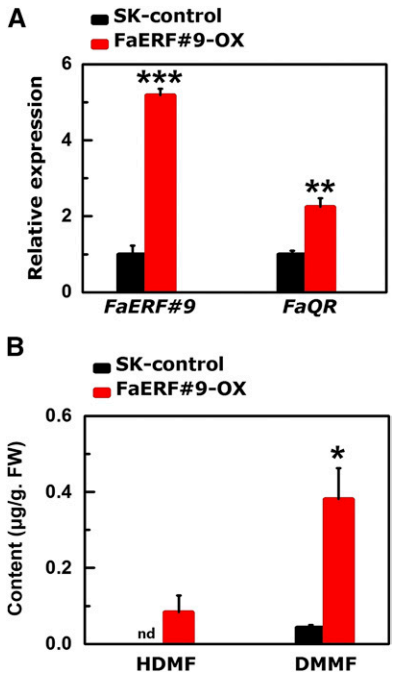

Figure 4. Transient overexpression (OX) of *FaERF#9* in strawberry fruit. A, Relative expression of *FaQR* and *FaERF#9* in *FaERF#9*-OX fruit 7 d after infiltration. The expression was calculated relative to the average value in control (SK) fruits. B, HDMF and DMMF contents in *FaERF#9*-OX fruit. The contents of both furanones were quantified using the peak area of the internal standard (2-octanol) as the reference. SE values were calculated from three replicates. Statistical significance was determined by Student's two-tailed *t* test (*, $P < 0.05$; **, $P < 0.01$; and ***, $P < 0.001$). FW, Fresh weight; nd, undetected.

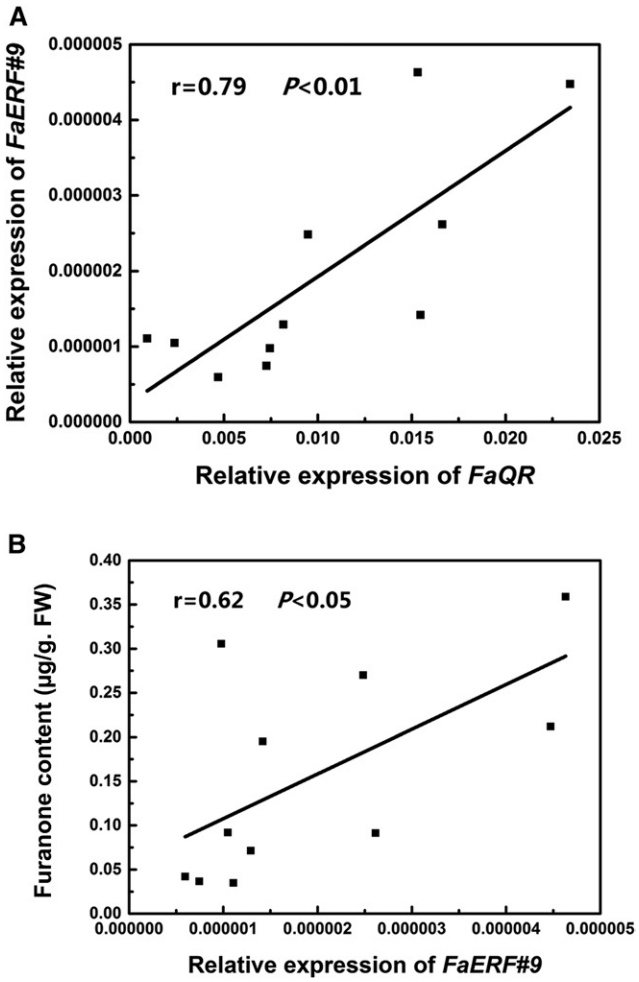

Figure 5. Scatterplots of 11 strawberry cultivars. A, Linear regression analysis between *FaERF#9* expression and *FaQR* expression. B, Linear regression analysis between *FaERF#9* expression and furanone content. The relative expression was normalized to that of the housekeeping gene *FaRIB413*, and furanone content was calculated with an internal standard as the reference. Significant differences were determined by SPSS Statistics 20.0. FW, Fresh weight.

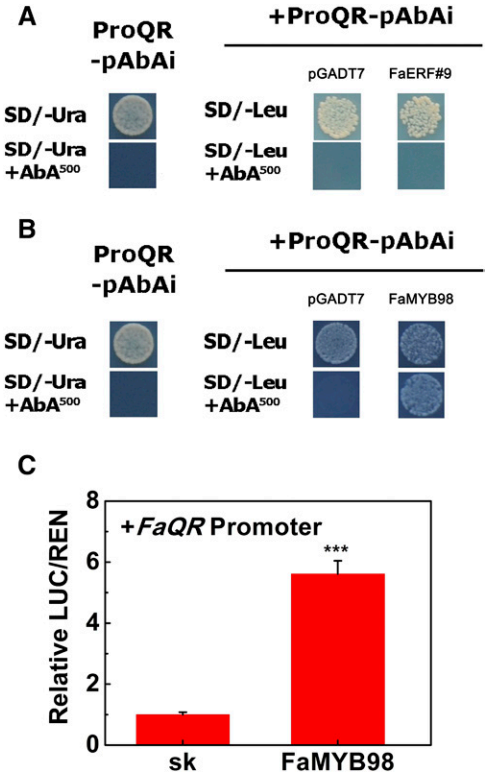

Figure 6. Interactions of FaERF#9 and FaMYB98 with the *FaQR* promoter. A, Yeast one-hybrid analysis of the interaction of FaERF#9 and the *FaQR* promoter. B, Yeast one-hybrid analysis of the interaction of FaMYB98 and the *FaQR* promoter. C, Regulatory effect of FaMYB98 on the *FaQR* promoter. Autoactivation was tested on SD/-Ura (synthetically defined medium without uracil) in the presence of aureobasidin A (AbA), and physical interaction was determined on SD/-Leu (synthetically defined medium without Leu) in the presence of AbA. LUC/REN values of the empty vector on the *FaQR* promoter were used as the calibrator, set as 1, and error bars were calculated from five replicates. Statistical significance was determined by Student's two-tailed *t* test (***, $P < 0.001$).

assay indicated that FaERF#9 cannot bind directly to the *FaQR* promoter (Fig. 6). This led us to speculate that activation may occur via a transcription complex involving an additional, as yet unknown regulator that can bind directly to the *FaQR* promoter.

In parallel with the investigation of the *FaAP2/ERF* genes, a cDNA library screening was performed with a yeast one-hybrid assay using the promoter of *FaQR* as the bait. This screen identified several transcription factors that could bind physically to the *FaQR* promoter, but only one MYB could activate transcription from the *FaQR* promoter (approximately 5.6-fold) relative to the control (Fig. 6) in the dual-luciferase assay. This MYB showed 44% amino acid identity with MYB98 (GenBank accession no. ABA42061.1), a transcriptional regulator in the synergid cells in Arabidopsis (Kasahara et al., 2005), and it was designated as FaMYB98. The specificity of FaMYB98 binding to the *FaQR* promoter was confirmed by electrophoretic mobility shift assay (EMSA; Fig. 7), and increasing the concentration of the cold probe reduced binding. In addition, mutating the putative binding sites (Gómez-Maldonado et al., 2004; Punwani et al., 2007), as shown in Figure 7, eliminated FaMYB98 protein binding. When the combined effect of FaERF#9 and FaMYB98 was analyzed (Fig. 8), a synergistic 14-fold activation of the *FaQR* promoter was observed, compared with the activation by either FaERF#9 or FaMYB98, which alone promoted transactivation 3.9- and 4.5-fold, respectively. In addition, overexpression of both genes (FaERF#9-FaMYB98-SK) in strawberry fruits resulted in higher expression of *FaERF#9* transcripts and higher furanone content than overexpression of *FaERF#9* (Supplemental Fig. S4; Supplemental Table S3). Subcellular localization analysis revealed that FaMYB98 also was localized in the nucleus (Supplemental Fig. S5).

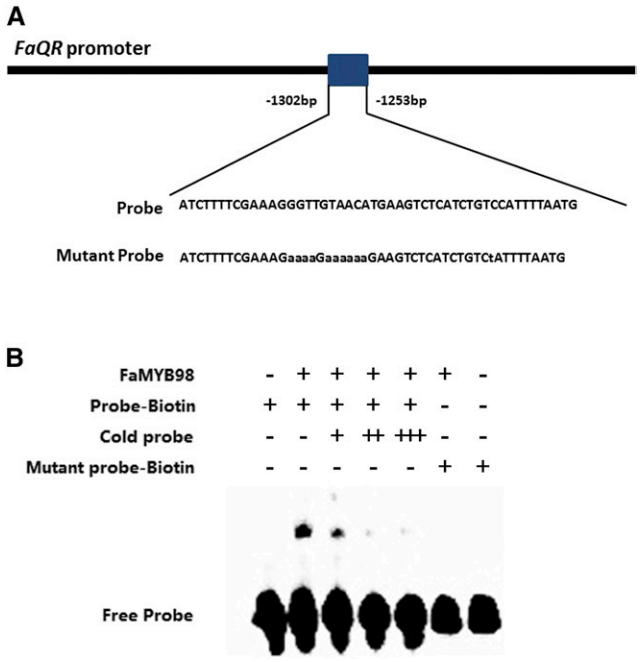

Figure 7. EMSA of FaMYB98 binding to the *FaQR* promoter. A, The probe sequence used for EMSA, and mutated nucleotides indicated with lowercase letters. B, Purified DNA-binding domain of FaMYB98 protein and biotin-labeled DNA probe were mixed and analyzed on 6% (m/v) native polyacrylamide gels and then photographed. The presence or absence of specific probes is marked by the symbol + or −.

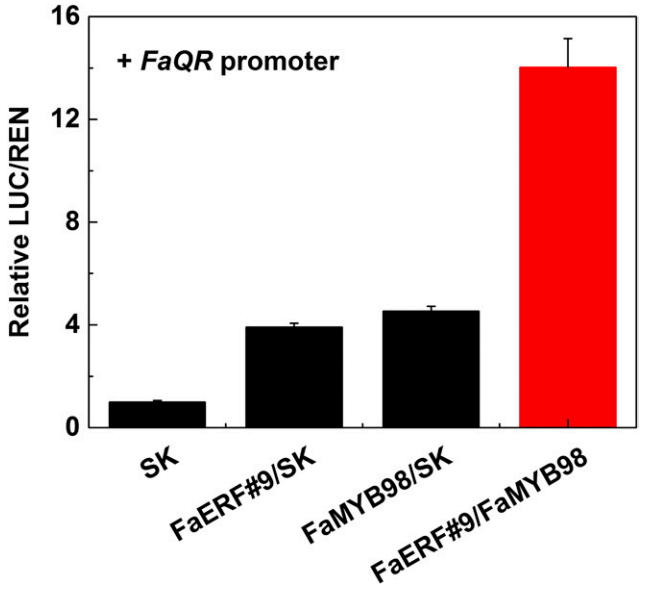

Figure 8. Combined activation effects of FaERF#9/FaMYB98 on the *FaQR* promoter. LUC/REN values obtained with the empty vector and the *FaQR* promoter were used as the calibrator, set as 1, and error bars were calculated from five replicates.

To investigate the potential interactions between FaERF#9 and FaMYB98, the DUALhunter system was used (Fig. 9). Cells expressing the FaMYB98 and FaERF#9 protein pair, using either FaMYB98 or FaERF#9 as the bait, grew on DDO, QDO, and QDO supplemented with 1 mM 3-AT selective medium, indicating interaction between the two proteins. This putative protein-protein interaction was confirmed by bimolecular fluorescence complementation (BiFC) assay, and the combinations FaMYB98-YFP^N/FaERF#9-YFP^C and FaERF#9-YFP^N/FaMYB98-YFP^C exhibited strong coincident signals in the nucleus, while negative controls produced no detectable fluorescence signal (Fig. 10). In addition, coexpression of FaERF#9-YFP^N/FaERF#9-YFP^C as well as FaMYB98-YFP^N/FaMYB98-YFP^C also generated signals in the nucleus, indicating that FaERF#9 and FaMYB98 both could form homodimers or possibly multimers in the nucleus (Fig. 10).

DISCUSSION

The AP2/ERF Superfamily in Strawberry

The AP2/ERF superfamily of plant transcription factors is defined by the AP2/ERF domain and comprises the ERF, AP2, and RAV families as well as one soloist member (Riechmann et al., 2000; Weirauch and

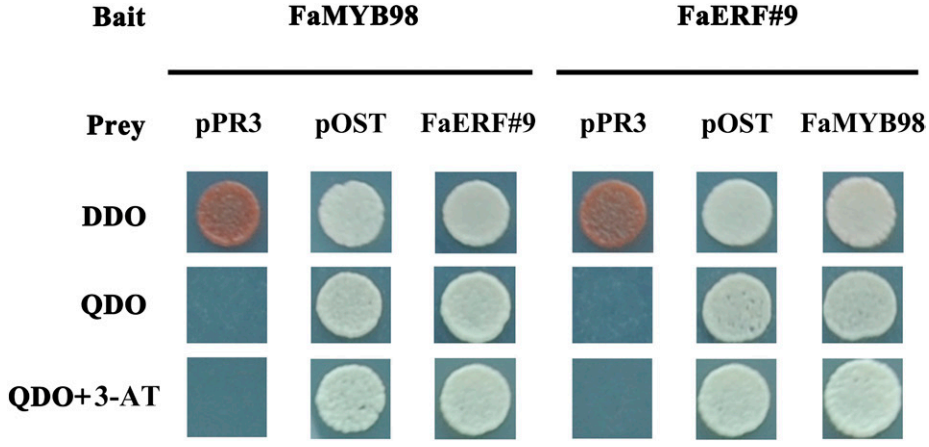

Figure 9. Yeast two-hybrid analysis of the protein-protein interactions between FaMYB98 and FaERF#9. Positive interactions were determined by the growth of yeast cells on selection plates. Bait with pOST acted as positive controls, and bait with pPR3 acted as negative controls. DDO, Synthetically defined medium without Trp and Leu; QDO, synthetically defined medium without Trp, Leu, His, and adenine; QDO+3-AT, QDO medium supplemented with 1 mM 3-amino-1,2,4-triazole.

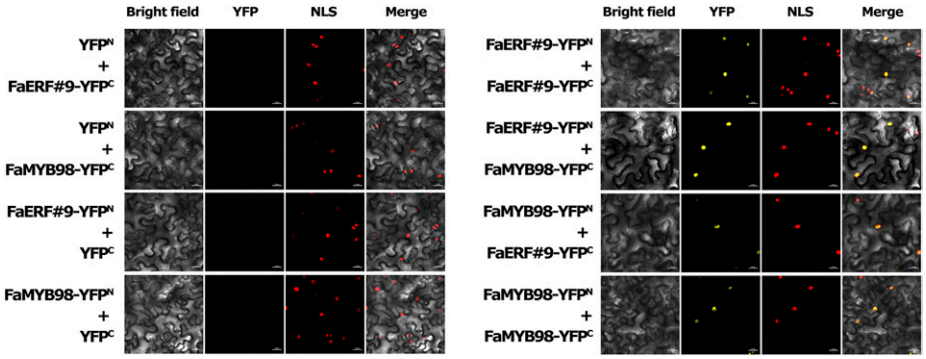

Figure 10. BiFC analysis of the protein-protein interactions between FaMYB98 and FaERF#9. The pairs of fusion proteins tested were FaMYB98-YFP^N+FaERF#9-YFP^C, FaERF#9-YFP^N+FaMYB98-YFP^C, FaMYB98-YFP^N+FaMYB98-YFP^C, and FaERF#9-YFP^N+-FaERF#9-YFP^C. The other combinations were negative controls. The tobacco used in the assay was stably transformed with a specific nucleus-localized red fluorescent protein construct, and the red fluorescence indicated the nucleus-localized signal (NLS). The fluorescence of the yellow fluorescent protein (YFP) visualized the interaction in vivo. Bars = 25 μm.

Hughes, 2011). The completion of multiple plant genome sequences has enabled a genome-scale analysis of the AP2/ERF family, which, in recent years, has been studied systematically in diverse fruit species such as tomato, grape, peach (*Prunus persica*), and kiwi fruit (*Actinidia deliciosa*; Zhuang et al., 2009; Licausi et al., 2010; Sharma et al., 2010; Yin et al., 2010; Pirrello et al., 2012; Zhang et al., 2012, 2016). A few *AP2/ERF* genes have been isolated and characterized in strawberry, and *CBF* orthologs (Owens et al., 2002; Koehler et al., 2012; Zhang et al., 2014) have been identified from different strawberry cultivars in several independent studies. Although they have distinct names, such as strawberry *CBF1* (*FaCBF1*), *FaCBF4* (GenBank accession no. HQ910515.1), and *CBF1* (GenBank accession no. EU117214.2), according to the phylogenetic tree generated in this study, the orthologs of *CBF1/CBF4/CBF2/CBF3* in Arabidopsis are similar to each other and to *FaERF#20* (Supplemental Fig. S1; Owens et al., 2002; Koehler et al., 2012; Zhang et al., 2014). *FaERF#20* has 85% sequence similarity with *FaCBF1*, identified by Owens et al. (2002); 93% similarity with *FaCBF4*, amplified by Koehler et al. (2012); and 75% similarity with *CBF1*, cloned by Zhang et al. (2014). The *AP2/ERF* genes characterized in other studies (Jia et al., 2011; Gao et al., 2015; Chai and Shen, 2016; Mu et al., 2016) also are noted in Supplemental Table S1.

Based on the computational analysis, we have identified a total of 120 *AP2/ERF* genes in octoploid strawberry (Supplemental Table S1). The number of predicted *AP2/ERF* genes (120) is comparable to those observed in other fruits, including tomato (112), Chinese plum (*Prunus salicina*; 116), *Citrus* spp. (126), and peach (131), but lower than those reported for grape (149; Xie et al., 2016). As shown in Supplemental Table S2, 79% (95 genes) of the *AP2/ERF* genes belong to the ERF family in strawberry, constituting the largest subfamily. The members of this subfamily can be classified into 10 groups (groups I–X) according to their sequence similarities to the Arabidopsis ERF genes (Nakano et al., 2006). The AP2 family encompasses the same number of genes in Arabidopsis, *Citrus* spp., and strawberry (18; Nakano et al., 2006; Xie et al., 2014), and there are six RAV genes in strawberry that are highly conserved in dicots such as grape, Arabidopsis, and *Populus trichocarpa* (Licausi et al., 2010).

Role of FaERF#9 in Regulating the Biosynthesis of HDMF: A Positive Regulator Acting in an Indirect Manner

The large-scale screening of the AP2/ERF superfamily in strawberry led to the identification of 11 ERFs and one RAV that transactivated the *FaQR* promoter more than 2-fold, with the highest activation caused by FaERF#9, which transactivated the *FaQR* promoter (Fig. 2) as well as up-regulating *FaQR* expression and furanone production in transient overexpression assays (Fig. 4), which have been used extensively to explore the fruit-associated gene functions in strawberry (Han et al., 2015; Medina-Puche et al., 2015; Vallarino et al., 2015; Carvalho et al., 2016; Song et al., 2016; Wang et al., 2018). *FaERF#9* transcripts accumulate in the fruit apical section before the basal section (Fig. 3), a finding consistent with the actual changes in furaneol content (Fig. 1) and the expression of *FaQR* (Fig. 1). The association between FaERF#9 transcripts and the accumulation of furanones also was established with different strawberry cultivars. The correlation between *FaERF#9* and *FaQR* expression as well as furanone content among cultivars supports a positive role of FaERF#9 in regulating furanone content (Fig. 5). These results indicate that *FaERF#9* transcript abundance may be a good indicator of the abundance of these important flavor volatiles in fruits of different cultivars. This should be considered as a method for high-throughput variety screening to replace direct measurement of volatiles.

FaERF#9 is a member of the ERF group II family and is most closely related to the Arabidopsis genes *At1g44830* (*ATERF014*), *At1g21910* (*DREB26*), and *At1g77640* (Supplemental Fig. S1). *At1g44830* was

observed to be strongly up-regulated in a comprehensive microarray analysis of the root transcriptome following NaCl exposure (Jiang and Deyholos, 2006). *At1g21910* (*DREB26*) was characterized functionally as a transactivator localized in the nucleus, exhibiting tissue-specific expression and participating in plant developmental processes as well as biotic and/or abiotic stress signaling (Krishnaswamy et al., 2011). However, none of these genes have been reported as furanone regulators. In strawberry, another five genes (*FaERF#6*, *FaERF#7*, *FaERF#8*, *FaERF#10*, and *FaERF#11*) also belong to the same group, with FaERF#8 also showing somewhat weaker activation activity toward the *FaQR* promoter than FaERF#9. The fact that FaERF#9 could not bind directly to the promoter of *FaQR* (Fig. 6) indicates that it might function as an indirect regulator of *FaQR* and furaneol biosynthesis.

A FaERF#9 and FaMYB98 Complex Is Involved in Regulating *FaQR* and Furaneol Biosynthesis

The findings that FaERF#9 could interact with FaMYB98 protein (Figs. 9 and 10) and that FaMYB98 could bind physically to the *FaQR* promoter (Figs. 6 and 7) provide evidence for a regulatory mechanism whereby FaERF#9 regulates *FaQR* and furaneol production as part of a complex with an MYB transcription factor. Since co-overexpression of *FaERF#9* and *FaMYB98* resulted in much higher activation activity toward *FaQR*, we speculate that FaERF#9 may recruit FaMYB98 homologs in tobacco to activate the *FaQR* promoter (Fig. 8). *FaOMT* is another key gene for furanone biosynthesis and a potential target for transcriptional activation. However, *FaERF#9* did not significantly activate the *FaOMT* promoter in a dual-luciferase assay, and the transcript level of *FaOMT* in the *FaERF#9*-overexpressing fruits showed no significant difference from that in the control (Supplemental Figs. S6 and S7). The *FaOMT* promoter was induced significantly by FaMYB98, but no synergistic effect of FaERF#9 and FaMYB98 on the promoter was observed (Supplemental Fig. S6). In previous studies of the regulation of plant volatile compounds, MYBs have been characterized as being involved mainly in the regulation of the benzenoid/phenylpropanoid pathway that produces floral volatiles in petunia (*Petunia hybrida*) and eugenol in ripe strawberry fruit (Verdonk et al., 2005; Colquhoun et al., 2011; Dal Cin et al., 2011; Spitzer-Rimon et al., 2012; Medina-Puche et al., 2015), but their role in the formation of volatiles from other pathways has not been reported. Our study demonstrates a role for MYB in the synthesis of furaneol, a carbohydrate-derived volatile compound, and reveals the synergistic interactions between an MYB and ERF in a transcription complex (Figs. 8–10).

Recent research has provided evidence for interactions between AP2/ERF and MYB transcription factors in regulating other aspects of fruit quality, including texture (EjAP2-1 and EjMYB; Zeng et al., 2015) and color (PyERF3 and PyMYB114; Yao et al., 2017). A group VIII ERF also was shown recently to interact with an MYB to regulate floral scent production in petunia (Liu et al., 2017). In strawberry fruit, DOF, in combination with an MYB, has been reported to be involved in the regulation of eugenol production, and the identification of this second transcription factor (DOF) suggests that it is a good target in breeding for improved flavor (Molina-Hidalgo et al., 2017; Tieman, 2017). Considering its important contribution to flavor in strawberry and many other highly valued fruit crop species (pineapple, tomato, mango, etc.), very little is known about the regulation of furaneol synthesis. Here, we established the role of FaERF#9 in the regulation of HDMF synthesis by direct protein-protein interactions with FaMYB98 to synergistically transactivate *FaQR*. The functional identification of this complex enhances our knowledge of the regulation of volatile compound synthesis and identifies a new AP2/ERF-MYB complex. Further examination of the other ERFs that stimulated transcription from the *FaQR* promoter (Fig. 2) may provide additional information about the complexity of this regulation. Overall, this study provides important clues for understanding the transcriptional regulation of HDMF synthesis and identifies specific transcription factors that are likely to be good targets for molecular breeding for improved flavor.

CONCLUSION

Screening of the AP2/ERF superfamily in strawberry identified candidate members capable of activating the *FaQR* promoter. An ERF transcription factor was identified as a positive regulator of HDMF synthesis in strawberry fruit, and the mechanism of activation was shown to involve an ERF-MYB transcription complex that regulates the transcription of *FaQR*, leading to the biosynthesis of HDMF, the characteristic volatile compound that has a major influence on strawberry aroma.

MATERIALS AND METHODS

Plant Materials and Growth Conditions

The strawberry (*Fragaria* × *ananassa* 'Yuexin', an octoploid cultivar) fruits used in this study were bred by the Zhejiang Academy of Agricultural Sciences in Haining, Zhejiang province, China. Fruits at various developmental and ripening stages, including G, T, IR, and R, were harvested (Fig. 1) and transported to the laboratory within 2 h. Thirty-six fruits of uniform size and free of visible defects were selected at each stage, with 12 fruits in each biological replicate. After removing the calyces, fruits were then divided into the basal and apical sections, which were sampled separately (Fig. 1). They were rapidly cut into pieces, frozen immediately in liquid nitrogen, and stored at −80°C until use. Red ripe fruits of different strawberry cultivars (octoploid cultivars), including cv Yueli, Benihoppe, Mengxiang, Amaou, 10-1-4, Akihime, Sweet Charlie, 07-1-4, Darselect, Yuexin, and Xuemei, also were provided by the Zhejiang Academy of Agricultural Sciences. For each cultivar, the fruits of three biological replicates were sampled, frozen in liquid nitrogen, and stored at −80°C for further use.

Tobacco plants (*Nicotiana benthamiana*) used for dual-luciferase assays and subcellular localization analysis in this study were grown in a growth chamber with a light/dark cycle of 16 h/8 h at 24°C.

Detection of DMMF and HDMF

Automated Headspace solid -phase microextraction was performed to detect both furanones in cv Yuexin strawberry fruit (Zorrilla-Fontanesi et al., 2012). Samples were ground into a powder under liquid nitrogen for analysis.

For the detection of DMMF (Fig. 1), 0.5 g (fresh weight) of each sample was weighed in the vial, to which was added 1 mL of EDTA solution (100 mM, pH 7.5), 1 mL of $CaCl_2$ solution (m/v = 20%), and 20 µL of 2-octanol as the internal standard (0.07 µg µL^{-1}). The mixture was homogenized, and the vial was closed and placed on the sample tray for analysis by a CombiPAL autosampler (CTC Analytic). The fruit volatiles were sampled by headspace solid-phase microextraction with a 65-µm polydimethylsiloxane-divinylbenzene fiber. Initially, vials were preincubated at 50°C for 10 min under continuous agitation (500 rpm); then, volatiles were extracted for 30 min at the same temperature and agitation speed. After that, the fiber was desorbed in the GC injection port for 5 min in splitless mode. The 7890A GC chromatograph was equipped with a DB-5ms column (60 m × 250 µm × 1 µm; J&W Scientific), with helium as the carrier gas at a constant flow of 1.2 mL min^{-1}. The GC device was programmed at an initial temperature of 35°C for 2 min, with a ramp of 5°C min^{-1} up to 250°C, and held for 5 min. The injection port, interface, and MS source temperatures were 250°C, 260°C, and 230°C respectively. The ionization potential was set at 70 eV, recorded by a 5975B mass spectrometer (Agilent Technologies, J&W Scientific), and the scanning speed was seven scans per second. The same method was used to analyze HDMF and DMMF in fruits from different cultivars (Supplemental Fig. S3), except for the sample preparation procedure (Aragüez et al., 2013): briefly, 0.5 g (fresh weight) of powdered fruit was incubated at 30°C in a water bath for 5 min, then 2 mL of NaCl (m/v = 20%) and 20 µL of 2-octanol as the internal standard (0.07 µg µL^{-1}) were added and homogenized.

For the detection of HDMF (Fig. 1) and both furanones (Fig. 4; Supplemental Table S3), a liquid-injection system equipped with CTC Pal ALS was used. One gram (fresh weight) of powdered fruit and 2 mL of NaCl (m/v = 20%) were homogenized in a 10-mL tube, and 300 µL of CH_2Cl_2 and 20 µL of 2-octanol (0.766 µg µL^{-1}) as the internal standard were added to extract the volatiles; the mixture was then homogenized again. The tubes were stored at room temperature for 20 min and centrifuged at 12,000 rpm for 5 min. The subnatant was pipetted into a clean 1.5-mL tube, in which 20 mg of anhydrous sodium sulfate was added; the tube was left without shaking for 0.5 h. Then, 150 µL of the solution was transferred into a GC vial and placed on the sample tray as described above. Each sample (1 µL) was injected using the autosampler, and the analysis was accomplished by a 7890A GC-MS system (Agilent Technologies, J&W Scientific) equipped with a DB-WAX column (30 m × 0.25 mm × 0.25 µm; J&W Scientific). Helium (1.2 mL min^{-1}) was used as a carrier gas. The injection port (splitless injection mode), interface, and MS source temperatures were as described above. The oven temperature was set at 60°C for 4 min, then increased to 180°C at a rate of 4°C min^{-1} and maintained for 30 min. DMMF was identified by comparison of electron ionization mass spectra and retention time data with the data from the NIST/EPA/NIH mass spectral library (NIST-08 and Flavor). HDMF (Fig. 1) was identified and qualified by comparison with injected standard (Sigma). The quantitative analysis of both furanones (Fig. 4; Supplemental Table S3; Supplemental Fig. S3) was determined using the peak area of the internal standard as a reference based on total ion chromatogram.

RNA Isolation and RT-qPCR

Total RNA from strawberry samples was isolated in this study using the CTAB method (Chang et al., 1993). Genomic DNA contamination was eliminated by TURBO Dnase (Ambion), and 1 µg of RNA was used to obtain cDNA using an IScript cDNA Synthesis Kit (Bio-Rad). The synthesized cDNA was diluted with water (1:20), and 2 µL of diluted cDNA was used as the template for RT-qPCR. Reactions were performed in a total volume of 20 µL, consisting of 10 µL of SYBR PCR supermix (Bio-Rad), 1 µL of each primer (10 µM), 6 µL of diethyl pyrocarbonate-water, and 2 µL of diluted cDNA on a CFX96 instrument (Bio-Rad; Yin et al., 2012). The oligonucleotide primers for RT-qPCR analysis of genes, including *AP2/ERF*, *FaQR*, and *FaOMT*, were designed according to the coding sequences of genes, and the specificity was verified before use (Min et al., 2012). NCBI/Primer-BLAST was applied to design the primers. Relative expression levels were normalized to that of an internal control, the interspacer 26S-18S strawberry RNA housekeeping gene *FaRIB413* (Zorrilla-Fontanesi et al., 2012). To investigate the differential expression of genes during fruit development and ripening stages, the relative expression of each gene at the R stage in the basal fruit section was set as 1 using the 2^{-nnCT} method. For transient overexpression assay, the relative expression of control fruits with an empty vector (SK) was set as 1. The primers used in RT-qPCR are listed in Supplemental Table S4.

Gene Isolation and Analysis

Multiple database searches were performed to identify members of the strawberry AP2/ERF superfamily in the published strawberry databases and annotations of strawberry and *Fragaria* × *vesca*, using the AP2/ERF DNA-binding domain as a query sequence, and 120 genes were identified with AP2/ERF domain(s). Based on the BLAST result, primers (listed in Supplemental Table S5) were used to amplify the coding full-length cDNAs of *AP2/ERF* genes. The deduced amino acid sequences of AP2/ERF proteins in Arabidopsis (*Arabidopsis thaliana*) used for the construction of a phylogenetic tree were obtained from The Arabidopsis Information Resource. Alignment of the proteins was performed using the neighbor-joining method in ClustalX (version 1.8.1), and the phylogenetic tree was constructed using FigTree (version 1.3.1).

FaMYB98 was obtained by yeast one-hybrid screening sequencing, and the full-length sequences were predicted by BLAST. Primers were designed (listed in Supplemental Table S5) to amplify the full-length coding sequence.

The promoter of *FaQR* was cloned by genome walking as described previously (Yin et al., 2010), and conserved cis-element motifs in the promoter were searched manually.

Conserved domains within the FaAP2/ERF proteins and FaMYB98 were analyzed by CD-search (https://www.ncbi.nlm.nih.gov/Structure/cdd/wrpsb.cgi), and cellular locations of proteins, including FaERF#9 and FaMYB98, were predicted with the WoLF PSORT program (https://www.genscript.com/wolf-psort.html).

Dual-Luciferase Assays

In accordance with a previous protocol (Yin et al., 2010), the full-length cDNAs of *FaAP2/ERF* or *FaMYB98* transcription factors were cloned into pGreen II 0029 62-SK vector, and the promoter of *FaQR* was cloned into pGreen II 0800-LUC vector. A luciferase gene from *Renilla* driven by a 35S promoter in the luciferase vector acted as a positive control. The above constructs were expressed transiently in tobacco (*Nicotiana benthamiana*) leaves by *Agrobacterium tumefaciens*-mediated infiltration (strain GV3101), and the activity of the transcription factors on the promoter was measured on day 3 after infiltration, indicated by the ratio of enzyme activities of LUC and REN using a Modulus Luminometer (Promega). To determine the activity of a specific transcription factor toward the promoter, we mixed the *A. tumefaciens* culture with 1 mL of transcription factor and 100 µL of promoter, and the LUC/REN value of the empty vector SK on the promoter was set as 1, as a calibrator. To test the combined effect of two transcription factors on the promoter, to the *A. tumefaciens* culture mixture we added 0.5 mL of each transcription factor and 100 µL of promoter; the effect of the mixtures that contained each transcription factor (0.5 mL) and empty vector SK (0.5 mL) also was tested on the promoter as a control.

Subcellular Localization Analysis

35S-FaERF#9-GFP and 35S-FaMYB98-GFP were expressed transiently in tobacco leaves by *A. tumefaciens* infiltration (EHA105) using the same method as described for the dual-luciferase assay above. The transiently infected leaves were imaged on day 3 after infiltration using a Nikon A1-SHS confocal laser scanning microscope. The excitation wavelength for GFP fluorescence was 488 nm, and fluorescence was detected at 490 to 520 nm. The primers used for GFP construction are listed in Supplemental Table S6.

Transient Overexpression in Strawberry Fruit

Transient overexpression of *FaERF#9* and an overexpression binary vector (pGreen II 0029 62-SK-FaERF#9-FaMYB98) was performed in strawberry fruit using the *FaERF#9*-SK construct described above for the dual-luciferase assays and the binary vector constructed according to Liu et al. (2013). The transfection of fruit was carried out at the G stage (Hoffmann et al., 2006). The *FaERF#9*-SK construct and binary vector were electroporated individually into *A. tumefaciens* GV3101, and the *A. tumefaciens* culture suspended in infiltration buffer was infiltrated into the whole fruit using a syringe. As a control treatment, fruits were infiltrated with *A. tumefaciens* carrying an empty vector SK

under the same transfection conditions. Fruits were left attached to the plants and harvested on day 7 after infiltration. Fruits of three biological replicates were sampled for further analysis.

Yeast One-Hybrid Assay

In order to identify proteins that bind to the *FaQR* promoter, the Matchmaker Gold Yeast One-Hybrid Library Screening System (Clontech) was used. The sequence of the *FaQR* promoter was cloned into the pAbAi vector, and the construct was integrated into the genome of the Y1HGold yeast strain. A mixture of total RNA from strawberry fruit at four stages (G, T, IR, and R) was used to construct the prey cDNA library (TaKaRa). The background AbA^r expression of the Y1HGold FaQR-pAbAi strain was tested according to the system user manual, and then screening for protein-DNA interactions was carried out. Furthermore, the full length of each transcription factor was cloned separately into pGADT7 AD vector to confirm the screening results. The relationship between FaERF#9 and the *FaQR* promoter also was examined individually. Primers used in this assay are listed in Supplemental Table S6.

Expression and Purification of FaMYB98 Recombinant Protein

A 405-bp region spanning the DNA-binding domain of FaMYB98 was amplified from FaMYB98 cDNA and cloned into a pET6×HN vector (Clontech) to generate the recombinant N-terminal His-tagged protein; the primers used are listed in Supplemental Table S6. The resulting construct was sequenced and introduced into *Escherichia coli* strain Rosetta 2(DE3)pLysS (Novagen). Ten milliliters of the overnight culture was combined with 500 mL of Luria-Bertani liquid medium (100 μg mL^{-1} ampicillin and 34 μg mL^{-1} chloramphenicol) as described (Li et al., 2017b). Isopropyl *β*-D-1-thiogalactopyranoside was added to a final concentration of 1 mM, and the bacterial culture was incubated at 18°C at 150 rpm for 18 h. Then, the cells were harvested using a centrifuge and resuspended in 1× PBS buffer (Sangon Biotech), after which they were disrupted by sonication and the supernatant was purified using a HisTALON Gravity Column (Clontech) according to the user manual. The PD-10 Desalting column (GE Healthcare) was then used for buffer change and sample cleanup of proteins according to the gravity protocol. SDS-PAGE was performed, and the protein was visualized using Coomassie Brilliant Blue.

EMSA

A Lightshift Chemiluminescent EMSA kit (Thermo) was used to perform EMSA experiments according to the manufacturer's instructions. Single-strand oligonucleotides were synthesized and biotinylated by GeneBio Biotech. The details of the EMSA are provided by Ge et al. (2017). The probes used for EMSAs are listed in Supplemental Table S6.

Yeast Two-Hybrid Assay

The DUALhunter system (Dualsystems Biotech) was used to investigate the interaction between FaERF#9 and FaMYB98. Full-length coding sequences of *FaERF#9* and *FaMYB98* were cloned into pDHB1 bait vector and pPR3-N prey vector, respectively, sequences were verified, and the bait plasmid was cotransformed with prey plasmid into NMY51 in the following combinations: FaMYB98-pDHB1/pPR3-N, FaMYB98-pDHB1/FaERF#9-pPR3-N, FaMYB98-pDHB1/pOst1-NubI, FaERF#9-pDHB1/pPR3-N, FaERF#9-pDHB1/FaMYB98-pPR3-N, and FaERF#9-pDHB1/pOst1-NubI (Li et al., 2017a). Transformed cells were spread onto the following plates: DDO (SD medium-Trp-Leu), QDO (SD medium-Trp-Leu-His-Ade), and QDO+3-AT (QDO medium supplemented with 1 mM 3-amino-1,2,4-triazole). The control plasmid pOst1-NubI was used to determine whether the bait was functional, the pPR3-N prey vector plasmid was used to test whether the bait displayed nonspecific background, and positive interactions were indicated by the growth of yeast on QDO and QDO+3-AT plates. The primers used in the DUALhunter assay are listed in Supplemental Table S6.

BiFC Assays

Full-length FaERF#9 and FaMYB98 were cloned into sequences encoding the N- and C-terminal fragments, respectively, of YFP (Lv et al., 2014). All constructs were expressed transiently in tobacco leaves by *A. tumefaciens* infiltration (EHA105). The YFP fluorescence of transfected leaves was imaged 40 h after infiltration by using a Nikon A1-SHS confocal laser scanning microscope. The excitation wavelength for YFP was 488 nm, and fluorescence was detected at 520 to 540 nm. Primers used are listed in Supplemental Table S6.

Statistics

Student's two-tailed *t* test (*, $P < 0.05$; **, $P < 0.01$; and ***, $P < 0.001$) was used to determine significant differences between two groups in this study. Microsoft Excel was used to perform linear regressive analysis, significant differences were determined by SPSS Statistics 20.0, and scatterplots were prepared with Origin8.0. LSD at the 5% level was calculated using Microsoft Excel. Figures were prepared with Origin8.0 (Microcal Software). The online tool MetaboAnalyst 3.6 (http://www.metaboanalyst.ca/) was used to analyze the transcript abundance of the *AP2/ERF* genes.

Accession Numbers

Sequence data from this article have been deposited in GenBank under the accession numbers MH332903 to MH333022 for AP2/ERF genes in strawberry and MH333023 for *FaMYB98*. GenBank accession numbers for *FaQR* and *FaOMT* were AY158836.1 (Raab et al., 2006) and AF220491.2 (Wein et al., 2002).

Supplemental Data

The following supplemental materials are available.

Supplemental Figure S1. Phylogenetic analysis of FaAP2/ERF and Arabidopsis AP2/ERF proteins.

Supplemental Figure S2. Analysis of *FaAP2/ERF* gene expression patterns in strawberry fruit during development and ripening.

Supplemental Figure S3. Contents of furanones in fruit of strawberry cultivars.

Supplemental Figure S4. Relative expression of *FaERF#9* in *FaERF#9-FaMYB98-* and *FaERF#9*-overexpressing fruits.

Supplemental Figure S5. Subcellular localization of FaMYB98.

Supplemental Figure S6. Combined activation effects of FaERF#9/FaMYB98 on the *FaOMT* promoter.

Supplemental Figure S7. Relative expression of *FaOMT* in *FaERF#9*-overexpressing fruits.

Supplemental Table S1. AP2/ERF superfamily genes in strawberry.

Supplemental Table S2. Classification of the AP2/ERF superfamily members in strawberry.

Supplemental Table S3. Furanone content in *FaERF#9-FaMYB98-* and *FaERF#9*-overexpressing fruits.

Supplemental Table S4. Primers used for RT-qPCR.

Supplemental Table S5. Primers used to amplify the full-length coding sequences of *AP2/ERF* genes and *FaMYB98* in strawberry.

Supplemental Table S6. Primers used for vector construction.

Received May 15, 2018; accepted June 30, 2018; published July 9, 2018.

LITERATURE CITED

Agarwal P, Agarwal PK, Joshi AJ, Sopory SK, Reddy MK (2010) Overexpression of PgDREB2A transcription factor enhances abiotic stress tolerance and activates downstream stress-responsive genes. Mol Biol Rep **37**: 1125–1135

Aragüez I, Osorio S, Hoffmann T, Rambla JL, Medina-Escobar N, Granell A, Botella MÁ, Schwab W, Valpuesta V (2013) Eugenol production in achenes and receptacles of strawberry fruits is catalyzed by synthases exhibiting distinct kinetics. Plant Physiol **163**: 946–958

Carvalho RF, Carvalho SD, O'Grady K, Folta KM (2016) Agroinfiltration of strawberry fruit: a powerful transient expression system for gene validation. Curr Plant Biol **6**: 19–37

Chai L, Shen YY (2016) FaABI4 is involved in strawberry fruit ripening. Sci Hortic (Amsterdam) **210**: 34–40

Chang SJ, Puryear J, Cairney J (1993) A simple and efficient method for isolating RNA from pine trees. Plant Mol Biol Rep **11**: 113–116

Colquhoun TA, Kim JY, Wedde AE, Levin LA, Schmitt KC, Schuurink RC, Clark DG (2011) PhMYB4 fine-tunes the floral volatile signature of Petunia × hybrida through PhC4H. J Exp Bot **62**: 1133–1143

Dal Cin V, Tieman DM, Tohge T, McQuinn R, de Vos RCH, Osorio S, Schmelz EA, Taylor MG, Smits-Kroon MT, Schuurink RC, (2011) Identification of genes in the phenylalanine metabolic pathway by ectopic expression of a MYB transcription factor in tomato fruit. Plant Cell **23**: 2738–2753

Fu X, Cheng S, Zhang Y, Du B, Feng C, Zhou Y, Mei X, Jiang Y, Duan X, Yang Z (2017) Differential responses of four biosynthetic pathways of aroma compounds in postharvest strawberry (*Fragaria×ananassa* Duch.) under interaction of light and temperature. Food Chem **221**: 356–364

Gao LM, Zhang J, Hou Y, Yao YC, Ji QL (2015) RNA-Seq screening of differentially-expressed genes during somatic embryogenesis in *Fragaria* × *ananassa* Duch. 'Benihopp'. J Hortic Sci Biotechnol **90**: 671–681

Ge H, Zhang J, Zhang YJ, Li X, Yin XR, Grierson D, Chen KS (2017) EjNAC3 transcriptionally regulates chilling-induced lignification of loquat fruit via physical interaction with an atypical CAD-like gene. J Exp Bot **68**: 5129–5136

Gómez-Maldonado J, Avila C, Torre F, Cañas R, Cánovas FM, Campbell MM (2004) Functional interactions between a glutamine synthetase promoter and MYB proteins. Plant J **39**: 513–526

Han Y, Dang R, Li J, Jiang J, Zhang N, Jia M, Wei L, Li Z, Li B, Jia W (2015) SUCROSE NONFERMENTING1-RELATED PROTEIN KINASE2.6, an ortholog of OPEN STOMATA1, is a negative regulator of strawberry fruit development and ripening. Plant Physiol **167**: 915–930

Hoffmann T, Kalinowski G, Schwab W (2006) RNAi-induced silencing of gene expression in strawberry fruit (Fragaria × ananassa) by agroinfiltration: a rapid assay for gene function analysis. Plant J **48**: 818–826

Jetti RR, Yang E, Kurnianta A, Finn C, Qian MC (2007) Quantification of selected aroma-active compounds in strawberries by headspace solid-phase microextraction gas chromatography and correlation with sensory descriptive analysis. J Food Sci **72**: S487–S496

Jia HF, Chai YM, Li CL, Lu D, Luo JJ, Qin L, Shen YY (2011) Abscisic acid plays an important role in the regulation of strawberry fruit ripening. Plant Physiol **157**: 188–199

Jiang Y, Deyholos MK (2006) Comprehensive transcriptional profiling of NaCl-stressed Arabidopsis roots reveals novel classes of responsive genes. BMC Plant Biol **6**: 25

Kasahara RD, Portereiko MF, Sandaklie-Nikolova L, Rabiger DS, Drews GN (2005) *MYB98* is required for pollen tube guidance and synergid cell differentiation in *Arabidopsis*. Plant Cell **17**: 2981–2992

Klein D, Fink B, Arold B, Eisenreich W, Schwab W (2007) Functional characterization of enone oxidoreductases from strawberry and tomato fruit. J Agric Food Chem **55**: 6705–6711

Koehler G, Wilson RC, Goodpaster JV, Sønsteby A, Lai X, Witzmann FA, You JS, Rohloff J, Randall SK, Alsheikh M (2012) Proteomic study of low-temperature responses in strawberry cultivars (*Fragaria* × *ananassa*) that differ in cold tolerance. Plant Physiol **159**: 1787–1805

Krishnaswamy S, Verma S, Rahman MH, Kav NNV (2011) Functional characterization of four APETALA2-family genes (*RAP2.6*, *RAP2.6L*, *DREB19* and *DREB26*) in *Arabidopsis*. Plant Mol Biol **75**: 107–127

Kulkarni R, Chidley H, Deshpande A, Schmidt A, Pujari K, Giri A, Gershenzon J, Gupta V (2013) An oxidoreductase from 'Alphonso' mango catalyzing biosynthesis of furaneol and reduction of reactive carbonyls. Springerplus **2**: 494

Larsen M, Poll L (1992) Odour thresholds of some important aroma compounds in strawberries. Z Lebensm Unters Forsch **195**: 120–123

Li L, Luo Z, Huang X, Zhang L, Zhao P, Ma H, Li X, Ban Z, Liu X (2015) Label-free quantitative proteomics to investigate strawberry fruit proteome changes under controlled atmosphere and low temperature storage. J Proteomics **120**: 44–57

Li SJ, Yin XR, Wang WL, Liu XF, Zhang B, Chen KS (2017a) Citrus CitNAC62 cooperates with CitWRKY1 to participate in citric acid degradation via up-regulation of *CitAco3*. J Exp Bot **68**: 3419–3426

Li X, Xu Y, Shen S, Yin X, Klee H, Zhang B, Chen K, Hancock R (2017b) Transcription factor CitERF71 activates the terpene synthase gene *CitTPS16* involved in the synthesis of *E*-geraniol in sweet orange fruit. J Exp Bot **68**: 4929–4938

Licausi F, Giorgi FM, Zenoni S, Osti F, Pezzotti M, Perata P (2010) Genomic and transcriptomic analysis of the AP2/ERF superfamily in *Vitis vinifera*. BMC Genomics **11**: 719

Licausi F, Ohme-Takagi M, Perata P (2013) APETALA2/Ethylene Responsive Factor (AP2/ERF) transcription factors: mediators of stress responses and developmental programs. New Phytol **199**: 639–649

Liu F, Xiao Z, Yang L, Chen Q, Shao L, Liu J, Yu Y (2017) PhERF6, interacting with EOBI, negatively regulates fragrance biosynthesis in petunia flowers. New Phytol **215**: 1490–1502

Liu XF, Yin XR, Allan AC, Lin Wang K, Shi YN, Huang YJ, Ferguson IB, Xu CJ, Chen KS (2013) The role of *MrbHLH1* and *MrMYB1* in regulating anthocyanin biosynthetic genes in tobacco and Chinese bayberry (*Myrica rubra*) during anthocyanin biosynthesis. Plant Cell Tissue Organ Cult **115**: 285–298

Lv Q, Zhong Y, Wang Y, Wang Z, Zhang L, Shi J, Wu Z, Liu Y, Mao C, Yi K, (2014) SPX4 negatively regulates phosphate signaling and homeostasis through its interaction with PHR2 in rice. Plant Cell **26**: 1586–1597

Medina-Puche L, Molina-Hidalgo FJ, Boersma M, Schuurink RC, López-Vidriero I, Solano R, Franco-Zorrilla JM, Caballero JL, Blanco-Portales R, Muñoz-Blanco J (2015) An R2R3-MYB transcription factor regulates eugenol production in ripe strawberry fruit receptacles. Plant Physiol **168**: 598–614

Ménager I, Jost M, Aubert C (2004) Changes in physicochemical characteristics and volatile constituents of strawberry (cv. Cigaline) during maturation. J Agric Food Chem **52**: 1248–1254

Min T, Yin XR, Shi YN, Luo ZR, Yao YC, Grierson D, Ferguson IB, Chen KS (2012) Ethylene-responsive transcription factors interact with promoters of *ADH* and *PDC* involved in persimmon (*Diospyros kaki*) fruit de-astringency. J Exp Bot **63**: 6393–6405

Molina-Hidalgo FJ, Medina-Puche L, Cañete-Gómez C, Franco-Zorrilla JM, López-Vidriero I, Solano R, Caballero JL, Rodríguez-Franco A, Blanco-Portales R, Muñoz-Blanco J, (2017) The fruit-specific transcription factor FaDOF2 regulates the production of eugenol in ripe fruit receptacles. J Exp Bot **68**: 4529–4543

Mu Q, Wang BJ, Leng XP, Sun X, Shangguan LF, Jia HF, Fang JG (2016) Comparison and verification of the genes involved in ethylene biosynthesis and signaling in apple, grape, peach, pear and strawberry. Acta Physiol Plant **38**: 44

Nakano T, Suzuki K, Fujimura T, Shinshi H (2006) Genome-wide analysis of the ERF gene family in Arabidopsis and rice. Plant Physiol **140**: 411–432

Owens CL, Thomashow MF, Hancock JF, Iezzoni AF (2002) *CBF1* orthologs in sour cherry and strawberry and the heterologous expression of *CBF1* in strawberry. J Am Soc Hortic Sci **127**: 489–494

Pirrello J, Prasad BC, Zhang W, Chen K, Mila I, Zouine M, Latché A, Pech JC, Ohme-Takagi M, Regad F, (2012) Functional analysis and binding affinity of tomato ethylene response factors provide insight on the molecular bases of plant differential responses to ethylene. BMC Plant Biol **12**: 190

Pisarnitskii AF, Demechenko AG, Egorov IA, Gvelesiani RK (1992) Methylpentoses are possible precursors of furanones in fruits. Prikl Biokhim Mikrobiol **28**: 123–127

Punwani JA, Rabiger DS, Drews GN (2007) MYB98 positively regulates a battery of synergid-expressed genes encoding filiform apparatus localized proteins. Plant Cell **19**: 2557–2568

Pyysalo T, Honkanen E, Hirvi T (1979) Volatiles of wild strawberries, *Fragaria vesca* L., compared to those of cultivated berries, *Fragaria* × *ananassa* cv Senga Sengana. J Agric Food Chem **27**: 19–22

Raab T, López-Ráez JA, Klein D, Caballero JL, Moyano E, Schwab W, Muñoz-Blanco J (2006) *FaQR*, required for the biosynthesis of the strawberry flavor compound 4-hydroxy-2,5-dimethyl-3(2H)-furanone, encodes an enone oxidoreductase. Plant Cell **18**: 1023–1037

Riechmann JL, Heard J, Martin G, Reuber L, Jiang C, Keddie J, Adam L, Pineda O, Ratcliffe OJ, Samaha RR, (2000) *Arabidopsis* transcription factors: genome-wide comparative analysis among eukaryotes. Science **290**: 2105–2110

Roscher R, Herderich M, Steffen JP, Schreier P, Schwab W (1996) 2,5-Dimethyl-4-hydroxy-3[2H]-furanone 6′O-malonyl-β-D-glucopyranoside in strawberry fruits. Phytochemistry **43**: 155–159

Roscher R, Bringmann G, Schreier P, Schwab W (1998) Radiotracer studies on the formation of 2,5-dimethyl-4-hydroxy-3(2H)-furanone in detached ripening strawberry fruits. J Agric Food Chem **46**: 1488–1493

Schwab W (1998) Application of stable isotope ratio analysis explaining the bioformation of 2,5-dimethyl-4-hydroxy-3(2H)-furanone in plants by a biological Maillard reaction. J Agric Food Chem **46**: 2266–2269

Schwab W (2013) Natural 4-hydroxy-2,5-dimethyl-3(2H)-furanone (Furaneol®). Molecules **18**: 6936–6951

Schwab W, Roscher R (1997) 4-Hydroxy-3(2H)-furanones: natural and Maillard products. Recent Res Dev Phytochem **1**: 643–673

Schwieterman ML, Colquhoun TA, Jaworski EA, Bartoshuk LM, Gilbert JL, Tieman DM, Odabasi AZ, Moskowitz HR, Folta KM, Klee HJ, (2014) Strawberry flavor: diverse chemical compositions, a seasonal influence, and effects on sensory perception. PLoS ONE **9**: e88446

Sharma MK, Kumar R, Solanke AU, Sharma R, Tyagi AK, Sharma AK (2010) Identification, phylogeny, and transcript profiling of ERF family genes during development and abiotic stress treatments in tomato. Mol Genet Genomics **284**: 455–475

Shen SL, Yin XR, Zhang B, Xie XL, Jiang Q, Grierson D, Chen KS (2016) *CitAP2.10* activation of the terpene synthase *CsTPS1* is associated with the synthesis of (+)-valencene in 'Newhall' orange. J Exp Bot **67**: 4105–4115

Shigyo M, Ito M (2004) Analysis of gymnosperm two-AP2-domain-containing genes. Dev Genes Evol **214**: 105–114

Song C, Hong X, Zhao S, Liu J, Schulenburg K, Huang FC, Franz-Oberdorf K, Schwab W (2016) Glucosylation of 4-hydroxy-2,5-dimethyl-3(2H)-furanone, the key strawberry flavor compound in strawberry fruit. Plant Physiol **171**: 139–151

Spitzer-Rimon B, Farhi M, Albo B, Cna'ani A, Ben Zvi MM, Masci T, Edelbaum O, Yu Y, Shklarman E, Ovadis M, (2012) The R2R3-MYB-like regulatory factor EOBI, acting downstream of EOBII, regulates scent production by activating *ODO1* and structural scent-related genes in petunia. Plant Cell **24**: 5089–5105

Tieman D (2017) Transcriptional control of strawberry ripening: two to tango. J Exp Bot **68**: 4407–4409

Vallarino JG, Osorio S, Bombarely A, Casañal A, Cruz-Rus E, Sánchez-Sevilla JF, Amaya I, Giavalisco P, Fernie AR, Botella MA, (2015) Central role of *FaGAMYB* in the transition of the strawberry receptacle from development to ripening. New Phytol **208**: 482–496

Verdonk JC, Haring MA, van Tunen AJ, Schuurink RC (2005) *ODORANT1* regulates fragrance biosynthesis in petunia flowers. Plant Cell **17**: 1612–1624

Wang S, Song M, Guo J, Huang Y, Zhang F, Xu C, Xiao Y, Zhang L (2018) The potassium channel *FaTPK1* plays a critical role in fruit quality formation in strawberry (*Fragaria* × *ananassa*). Plant Biotechnol J **16**: 737–748

Wein M, Lavid N, Lunkenbein S, Lewinsohn E, Schwab W, Kaldenhoff R (2002) Isolation, cloning and expression of a multifunctional O-methyltransferase capable of forming 2,5-dimethyl-4-methoxy-3(2H)-furanone, one of the key aroma compounds in strawberry fruits. Plant J **31**: 755–765

Weirauch MT, Hughes TR (2011) A catalogue of eukaryotic transcription factor types, their evolutionary origin, and species distribution. *In* **TR Hughes**, ed, A Handbook of Transcription Factors. Springer, Dordrecht, The Netherlands, pp 25–73

Wüst M (2017) Biosynthesis of plant-derived odorants. *In* **A Buettner**, ed, Springer Handbook of Odor. Springer, Switzerland, pp 9–10

Xie XL, Shen SL, Yin XR, Xu Q, Sun CD, Grierson D, Ferguson I, Chen KS (2014) Isolation, classification and transcription profiles of the AP2/ERF transcription factor superfamily in citrus. Mol Biol Rep **41**: 4261–4271

Xie XL, Yin XR, Chen KS (2016) Roles of APETALA2/ethylene-response factors in regulation of fruit quality. Crit Rev Plant Sci **35**: 120–130

Yao G, Ming M, Allan AC, Gu C, Li L, Wu X, Wang R, Chang Y, Qi K, Zhang S, (2017) Map-based cloning of the pear gene *MYB114* identifies an interaction with other transcription factors to coordinately regulate fruit anthocyanin biosynthesis. Plant J **92**: 437–451

Yin XR, Allan AC, Chen KS, Ferguson IB (2010) Kiwifruit *EIL* and *ERF* genes involved in regulating fruit ripening. Plant Physiol **153**: 1280–1292

Yin XR, Shi YN, Min T, Luo ZR, Yao YC, Xu Q, Ferguson I, Chen KS (2012) Expression of ethylene response genes during persimmon fruit astringency removal. Planta **235**: 895–906

Zabetakis I, Holden MA (1997) Strawberry flavour: analysis and biosynthesis. J Sci Food Agric **74**: 421–434

Zabetakis I, Gramshaw JW, Robinson DS (1999) 2,5-Dimethyl-4-hydroxy-2*H*-furan-3-one and its derivatives: analysis, synthesis and biosynthesis—a review. Food Chem **65**: 139–151

Zeng JK, Li X, Xu Q, Chen JY, Yin XR, Ferguson IB, Chen KS (2015) *EjAP2-1*, an *AP2/ERF* gene, is a novel regulator of fruit lignification induced by chilling injury, via interaction with *EjMYB* transcription factors. Plant Biotechnol J **13**: 1325–1334

Zhang AD, Hu X, Kuang S, Ge H, Yin XR, Chen KS (2016) Isolation, classification and transcription profiles of the Ethylene Response Factors (ERFs) in ripening kiwifruit. Sci Hortic (Amsterdam) **199**: 209–215

Zhang CH, Shangguan LF, Ma RJ, Sun X, Tao R, Guo L, Korir NK, Yu ML (2012) Genome-wide analysis of the AP2/ERF superfamily in peach (*Prunus persica*). Genet Mol Res **11**: 4789–4809

Zhang Y, Tang HR, Luo Y, Wang XR, Chen Q, Liu ZJ (2014) Isolation and expression analysis of a CRT/DRE-binding factor gene *FaCBF1* from *Fragaria* × *ananassa*. Acta Hortic Sin 240–248

Zhu Q, Zhang J, Gao X, Tong J, Xiao L, Li W, Zhang H (2010) The *Arabidopsis* AP2/ERF transcription factor *RAP2.6* participates in ABA, salt and osmotic stress responses. Gene **457**: 1–12

Zhuang J, Peng RH, Cheng ZM, Zhang J, Cai B, Zhang Z, Gao F, Zhu B, Fu XY, Jin XF, (2009) Genome-wide analysis of the putative AP2/ERF family genes in *Vitis vinifera*. Sci Hortic (Amsterdam) **123**: 73–81

Zorrilla-Fontanesi Y, Rambla JL, Cabeza A, Medina JJ, Sánchez-Sevilla JF, Valpuesta V, Botella MA, Granell A, Amaya I (2012) Genetic analysis of strawberry fruit aroma and identification of *O-methyltransferase FaOMT* as the locus controlling natural variation in mesifurane content. Plant Physiol **159**: 851–870